

# Designability, thermodynamic stability, and dynamics in protein folding: a lattice model study

Régis Mélin<sup>(1),(2)</sup>, Hao Li<sup>(2),(3)</sup>, Ned S. Wingreen<sup>(2)</sup>, and Chao Tang<sup>(2)</sup>

<sup>(1)</sup> Centre de Recherches sur les Très basses températures\*(CRTBT-CNRS)  
Laboratoire conventionné avec l'Université Joseph Fourier  
BP 166X, 38042 Grenoble Cédex, France

<sup>(2)</sup> NEC Research Institute, 4 Independence Way, Princeton, NJ 08540, USA

<sup>(3)</sup> Center for Studies in Physics and Biology,  
Rockefeller University, 1230 York Avenue, New York, NY 10021, USA

## Abstract

In the framework of a lattice-model study of protein folding, we investigate the interplay between designability, thermodynamic stability, and kinetics. To be “protein-like”, heteropolymers must be thermodynamically stable, stable against mutating the amino-acid sequence, and must be fast folders. We find two criteria which, together, guarantee that a sequence will be “protein like”: i) the ground state is a highly designable structure, *i. e.* the native structure is the ground state of a large number of sequences, and ii) the sequence has a large  $\Delta/\Gamma$  ratio,  $\Delta$  being the average energy separation between the ground state and the excited compact conformations, and  $\Gamma$  the dispersion in energy of excited compact conformations. These two criteria are not incompatible since, on average, sequences whose ground states are highly designable structures have large  $\Delta/\Gamma$  values. These two criteria require knowledge only of the compact-state spectrum. These claims are substantiated by the study of 45 sequences, with various values of  $\Delta/\Gamma$  and various degrees of designability, by means of a Borst-Kalos-Lebowitz algorithm, and the Ferrenberg-Swendsen histogram optimization method. Finally, we report on the reasons for slow folding. A comparison between a very slow folding sequence, an average folding one and a fast folding one suggests that slow folding originates from a proliferation of nearly compact low-energy conformations, not present for fast folders.

---

\*U.P.R. 5001 du CNRS

# 1 Introduction

Among the set of all possible linear amino-acid heteropolymers, only very few are “protein like”. For a heteropolymer to be “protein like”, three requirements must be met: (i) The heteropolymer must be thermodynamically stable: at thermal equilibrium, it must spend a large fraction of its time in the ground state. (Anfissens [1] has shown the ground state of a protein to be the biologically active configuration.) (ii) The heteropolymer must have a fast folding time: the native state should be kinetically accessible, typically within milliseconds to seconds for real proteins. (iii) The “protein-like” heteropolymer must be stable against mutations: if an amino acid is mutated into another one, the native structure should typically be preserved.

Why are some sequences of amino acids “protein like” while others are not? Since theoretical methods cannot yet reliably find the ground state of real amino-acid chains, we address this question within a simple lattice model. Lattice models have been widely used in the study of protein folding dynamics [2, 3, 4, 5, 6, 7, 8]. The main ingredients of these lattice models are (i) the protein is viewed as a heteropolymer on a cubic lattice, and (ii) non-covalently-bonded nearest neighbor monomers experience an interaction that depends on monomer type. In one class of lattice models, the interactions between adjacent monomers are chosen as random variables from a continuous probability distribution (see for instance [3, 4, 6]). We adopt another approach, namely a so-called H-P model, where the monomers come in only two types, H(ydrophobic) or P(olar) [2, 7]. The main physical motivation for studying H-P models is that the specific ground-state configuration of real proteins appears to be largely determined by optimal burial of hydrophobic amino acids away from water[9]. It was also shown [10], from an analysis of the Miyazawa and Jernigan matrix [11], that the uncharged amino acids fall into two sets: hydrophobic and polar, according to their affinity for water. Moreover, there is experimental evidence that the native structures of certain proteins are stable when hydrophobic amino acids are substituted within the hydrophobic class and polar amino acids are substituted within the polar class[12]. The small number of possible interactions in an H-P model (H-H, H-P, and P-P) and the finite number of possible sequences of a given length provide realistic constraints on the design of particular structures. Li *et al.* [13] took advantage of these constraints to study some design properties of an H-P model in the complete space of possible sequences. In particular these authors introduced the concept of *designability*. In the terminology of Li *et al.*, the designability of a given compact structure is defined as the number  $N_S$  of sequences that have this structure as their nondegenerate compact ground state; a highly designable structure is the nondegenerate ground state of an atypically large number of sequences. These authors reached the conclusion that (i) highly designable structures are likely to be thermodynamically stable since they have a large gap in their compact state spectrum, (ii) highly designable structures are likely to be stable against point mutations, and (iii) highly designable structures have protein-like motifs. These observations suggest that Nature’s selection of protein structures is not accidental but a consequence

of thermodynamic stability and stability against mutations.

The aim of the present article is to push further the analysis of Li *et al.*. In particular, the study in [13] is limited to the compact-state spectra of H-P heteropolymers of 27 monomers length (the compact states of which fill a  $3 \times 3 \times 3$  cube), and the dynamical aspects are not discussed. Here we address thermodynamic and dynamic properties including all states, not only the compact ones. Of course, our present study is therefore limited to a small number of sequences (45), in contrast to the complete enumeration in [13]. More precisely, we address the following questions:

- (i) In the compact-state-spectrum studies, thermodynamic stability is measured by the gap in the compact-state spectrum. By gap, we mean the energy difference between the first excited compact state(s) and the ground compact state. How does the compact-state-spectrum gap correlate with the “true” thermodynamic stability where all the possible conformations (including the open and partially open ones) are taken into account? Also, how does the “true” thermodynamic stability correlate with the degree of designability?
- (ii) How does the folding time correlate with the compact-state spectrum? An answer to this question was postulated in [4]: a small gap in the compact-state spectrum leads to low foldability and a large gap in the compact-state spectrum leads to fast folders. It was shown in [6] that this postulate is *wrong* in the framework of a random interaction model: even though sequences with a large compact state gap are fast folders, sequences with a small compact state gap can fold either slow or fast. Is the postulate right or wrong for H-P heteropolymers?
- (iii) Are highly designable structures also fast folders? Sequences that have highly designable ground states and thus are stable against mutations are also typically thermodynamically stable according to the analysis of the compact-state spectrum carried out in Ref. [13]. Moreover, Vendruscolo *et al.* [14] showed, in different lattice models, that both types of stability are equivalent. One would like to know whether the requirement of fast folding dynamics introduces new constraints on the set of “protein-like” sequences. Finally, one can ask why are some sequences fast folders while others are slow?

This article is organized as follows: section 2 is devoted to the details of the model and the technical aspects of the simulations. We implement several techniques that were developed in the context of statistical mechanics of spin models. These techniques are next used in sections 3 and 4 to analyze the thermodynamics and dynamics of a set of sequences. Section 5 summarizes our answers to the questions presented above.

## 2 Model and simulation techniques

The aim of this section is to briefly recall the definition of the heteropolymer H-P model, and to describe the simulation techniques.

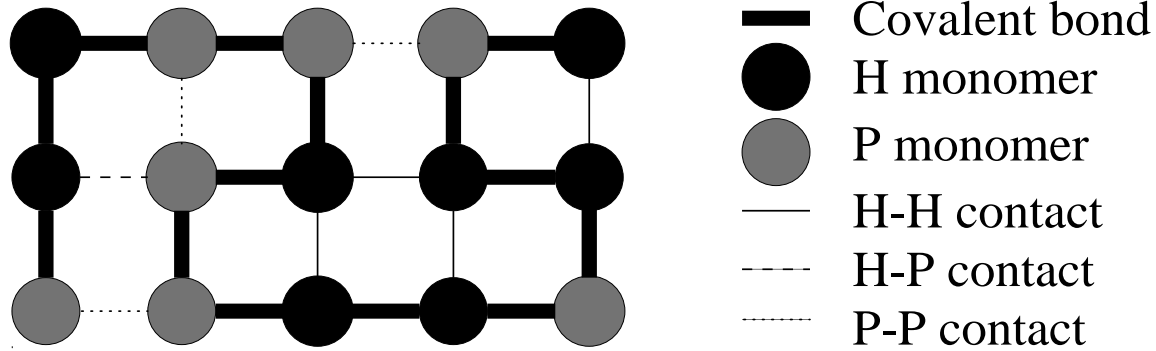


Figure 1: A conformation of a 15-mer in two dimensions.

## 2.1 The model

In the model analyzed in [13], a protein is a self-avoiding walk of monomers on a cubic lattice. A sequence is defined by the set  $\{\sigma_i\}$  of amino acids along the chain, where  $\sigma_i \in \{H(\text{hydrophobic}), P(\text{polar})\}$ , and  $i$  runs over the monomers along the chain ( $i = 1, \dots, 27$  for a chain which folds into a compact  $3 \times 3 \times 3$  cube). The different structures are defined by assigning a position  $\mathbf{r}_i$  to the  $i$ -th monomer on the cubic lattice, such that the distance between two consecutive monomers is equal to unity and two monomers cannot lie at the same site (self-avoidance condition). Given a sequence  $\sigma$ , the Hamiltonian is

$$H = \sum_{i < j} E_{\sigma_i, \sigma_j} \Delta(\mathbf{r}_i, \mathbf{r}_j), \quad (1)$$

where  $E_{H,H}$ ,  $E_{H,P}$ , and  $E_{P,P}$  are the energies of H–H, H–P, and P–P contacts, respectively, and  $\Delta(\mathbf{r}_i, \mathbf{r}_j) = 1$  if  $\mathbf{r}_i$  and  $\mathbf{r}_j$  are nearest-neighboring sites with  $i$  and  $j$  not adjacent along the chain, and zero otherwise. For instance, in the case of the two dimensional conformation of Fig. 1, there are 4 H–H contacts, 1 H–P contact, and 3 P–P contacts and the energy of this conformation is thus  $4E_{H,H} + E_{H,P} + 3E_{P,P}$ . The present model differs from the H–P models in [2, 7] since we take the interaction energies  $E_{H,H}$ ,  $E_{H,P}$ , and  $E_{P,P}$  to be all different from each other. From the analysis of the Miyazawa–Jernigan matrix for real proteins, it was shown in [10] that  $E_{H,H} < E_{H,P} < E_{P,P}$  and  $(E_{H,H} + E_{P,P})/2 < E_{H,P}$ . This last condition expresses the fact that different types of monomers tend to segregate. Following [13], we choose  $E_{H,H} = -2.3 - E_C$ ,  $E_{H,P} = -1 - E_C$  and  $E_{P,P} = -E_C$ . These dimensionless coefficients define the energy scale in which the temperature will be measured. An increase of the compactness energy  $E_C$  tends to favor compact conformations with respect to open ones. The results of [13] concerning the compact state spectrum are of course independent of  $E_C$ . In the present work, the open, partially open, and compact states are all taken into account in the numerical calculations, so that the results presented here depend on  $E_C$ . The determination of  $E_C$  from an analysis of the Miyazawa and Jernigan matrix along the lines of [10] is rather imprecise, but such an analysis suggests that  $E_C$  is of the order of 2 or 3. From the point of view of our

calculations, we have chosen the overall drive to compactification  $E_C$  to be large enough so that (i) the average compactification time (being the average time to first reach a compact state) is much smaller than the average folding time (being the average time to first reach the ground state) and (ii) very few sequences have a non-compact ground state. However,  $E_C$  should not be too large since, as was shown in [7], as  $E_C$  increases above a certain threshold, the folded phase gives way to a collapsed glassy phase. In practice, after preliminary simulations, we have chosen  $E_C = 1.5$ .

## 2.2 Simulation techniques

### 2.2.1 Dynamics

The most commonly used algorithm in three-dimensional lattice-heteropolymer folding dynamics is the Monte-Carlo algorithm with two one-monomer moves (end moves, corner moves) and one two-monomer move (crankshaft move) [see [7] for a pedagogical description of this algorithm]. However, for the model we simulated, this algorithm spends most of the time refusing moves, leading to large computation times. Hence, we chose to implement a Bortz-Kalos-Lebowitz (BKL) type algorithm [15], an algorithm especially efficient in the presence of slow relaxation. In contrast to the standard Monte-Carlo algorithm, this algorithm never rejects moves. In practice, one keeps track of all the possible states  $\alpha$  that can be reached after the three types of moves listed above, starting from a state  $\alpha_0$ . Once the list of all possible moves is established, together with the Monte-Carlo transition probabilities,

$$P_{\alpha_0 \rightarrow \alpha} = \text{Min} \left( \exp \left( -\frac{\Delta E_{\alpha_0 \rightarrow \alpha}}{T} \right), 1 \right), \quad (2)$$

one move is picked according to its relative transition probability and that move is then performed. The time spent in the state  $\alpha_0$  is randomly chosen from the exponential distribution

$$P(\tau_{\alpha_0}) = \exp \left( - \left( \sum_{\alpha \neq \alpha_0} P_{\alpha_0 \rightarrow \alpha} \right) \tau_{\alpha_0} \right). \quad (3)$$

One need not recalculate this list of possible final states at each step, but instead one updates this list by canceling moves that are no longer possible and adding new moves that become possible. The energy costs  $\Delta E_{\alpha_0 \rightarrow \alpha}$  of all these moves are also updated. This algorithm is especially efficient for slow and average folders, but still does not allow systematic studies at low temperatures. One unit time of this BKL algorithm (noted BKL unit in the following) corresponds to 27 Monte-Carlo-Steps (MCSs) of the usual Monte-Carlo algorithm (in lattice heteropolymer folding and for the usual Monte-Carlo algorithm, one MCS usually corresponds to attempting to move one monomer).

### 2.2.2 Thermodynamics

One possibility to compute thermodynamic quantities is to carry out an exhaustive enumeration of all the possible conformations, including the noncompact ones. Such an exact method was used for

instance in [6] in the case of a 15-mer in three dimensions, and in [14] for a 16-mer in two dimensions. Since, in practice, we could not apply this exact method to 27-mers in three dimensions, we have used Monte-Carlo histogram techniques to study the thermodynamics.

Several groups working on proteins have rediscovered the Monte-Carlo histogram technique and applied it to heteropolymer models of proteins. We refer the reader to [7] for a clear description of this technique. Most simply, the technique consists of carrying out a simulation at a given temperature  $T_0$  and keeping track of the histogram of various quantities, for instance the joint probability of the energy  $E$ , number of contacts, and similarity with the ground state. Using this histogram calculated at  $T_0$ , one can recalculate several thermodynamic quantities at another temperature  $T$  by changing the Boltzmann weight to  $\exp(-E/T)$  without carrying out a new simulation. However,  $T$  should remain close to  $T_0$  since the simulation at temperature  $T_0$  is carried out over a finite time and the phase space is thus only partially sampled. We did not in fact use this “naive” histogram technique but rather made use of the powerful method invented by Ferrenberg and Swendsen [16, 17]. This method consists in optimizing several histograms calculated at different temperatures to obtain the temperature dependence of various thermodynamic quantities. Moreover, the accuracy of the optimized thermodynamic quantities can be evaluated, and additional simulations can be carried out when necessary. Following [16], we briefly summarize this technique by focusing on the case of the single energy histogram, the generalization to joint histograms of various quantities being straightforward. We consider  $R$  energy histograms labeled by  $n = 1, \dots, R$ , carried out over  $t_n$  time units at the temperatures  $T_1, \dots, T_n, \dots, T_R$ , with the normalization

$$t_n = \sum_E N_n(E),$$

where  $N_n(E)$  is the number of times a state (or states) with energy  $E$  is sampled in the  $n$ -th histogram. The partition function  $Z(T)$  is expanded over the density of states  $W(E)$  as

$$Z(T) = \sum_E W(E) \exp(-E/T).$$

Each of the  $R$  histogram simulations carried out at a temperature  $T_n$  leads to a “naive” estimate of the density of states

$$W_n(E) = t_n^{-1} N_n(E) \exp(E/T_n - F_n/T_n), \quad (4)$$

with  $F_n$  the free energy at temperature  $T_n$ . The Ferrenberg and Swendsen method [16] consists in expanding the density of states  $W(E)$  as a combination of the “naive” densities of states (4)

$$W(E) = \sum_{n=1}^R p_n(E) W_n(E),$$

the coefficients of this expansion (as well as the free energies  $F_n$  in (4)) being determined by minimizing the error in this estimation of  $W(E)$ . The result is a closed set of multiple-histogram equations

for the  $F_n$  [16]

$$P(E, T) = \frac{\sum_{n=1}^R N_n(E) \exp(-E/T)}{\sum_{n=1}^R t_n \exp(-E/T_n + F_n/T_n)} \quad (5)$$

$$\exp(F_n/T_n) = \sum_E P(E, T_n). \quad (6)$$

Once (5) and (6) have been solved by successive iterations, the average of an energy-dependent operator is calculated as

$$\langle \mathcal{O}(E) \rangle = \frac{\sum_E \mathcal{O}(E) P(E, T)}{\sum_E P(E, T)}.$$

### 3 Thermodynamics

The compact state spectrum was previously determined by means of exact enumerations [13]. Thanks to this work, we know for each sequence the lowest energy compact state. However, it is possible that the true ground state is not compact. We therefore checked during the histogram calculations that no open state has a lower energy than the compact ground state. We eliminated a few sequences with noncompact ground states. Since we were not able to perform an exact enumeration of the noncompact states, we cannot exclude the possibility of a noncompact ground state that was not found during the simulations. However, we believe that this possibility is rather unlikely. We will comment later on the characteristics of those few sequences with a noncompact ground state.

#### 3.1 Qualitative study of a thermodynamically stable and unstable sequence

We first begin with a qualitative analysis of a “protein-like” and a “non-protein-like” sequence, from the point of view of thermodynamics. As stated in the introduction, one necessary condition for a sequence to be “protein-like” is that it be thermodynamically stable. Hence, we have to find a quantitative way to measure thermal stability. It has been proposed [18] that real proteins undergo a folding transition at some temperature  $T_f$  larger than the glass transition  $T_g$ , below which the dynamics dramatically freezes. For “protein-like” sequences, folding should be a first-order-like transition, with  $T_f$  much larger than  $T_g$ , thus allowing the possibility of a temperature regime in which the ground state is thermodynamically favored and kinetically accessible. By “first-order-like”, we mean that as a function of temperature the native state occupancy has a narrow transition from a low value in the unfolded phase to a high value in the folded phase. We will use the width of this transition as a measure of thermodynamic stability, the thermodynamically stable sequences having a narrow transition. The first-order-like behavior of the folding transition was put on a quantitative basis for a lattice H-P model by Soccia and Onuchic [7]. These authors studied the shape of the energy histogram and observed a transition from a unimodal shape to a bimodal shape as the temperature was lowered below  $T_f$ , suggesting the occurrence of a first-order-like transition.

On the other hand, in the case of a thermodynamically unstable sequence (and thus one that is not “protein-like”), there are low-lying states competing with the ground state, and the transition to the folded ground state as the temperature is decreased is thus broad. In order to compare different sequences, we measure thermodynamic stability in terms of the width in temperature of the transition to the native state compared to the transition temperature. In biological situations, the temperature is usually fixed and the notion of thermal stability is then not only sequence-dependent but also temperature-dependent. For instance, some sequences could have a narrow transition to the folded state but with too low a  $T_f$ , so that in practice, the protein is unfolded at the temperature of interest. Our definition of thermodynamic stability is thus, in the context of real proteins, only a necessary condition.

Following Socci and Onuchic [7], we employ the optimized histogram method described in section 2.2.2, and determine the probability  $\mathcal{P}_{25}(T)$  that the sequence is in any conformation having more than 25 correct ground-state contacts, or “native” contacts, out of 28 possible contacts for the fully folded structure. Throughout this paper, this set of conformations will be referred to as “native states”. We will consider a heteropolymer as correctly folded if the number of native contacts is larger than or equal to 25. This assumption speeds up computations and is sensible from the point of view of real proteins since structure fluctuations around the folded conformation are expected, and do not prevent the protein from being functional (see for instance [19]). The variation of  $\mathcal{P}_{25}(T)$  as a function of temperature  $T$  are shown on Fig. 2 for the thermodynamically stable sequence A and the thermodynamically unstable sequence C. [These two sequences will be studied in detail in the present article]. The larger width of the transition to the folded conformation in the case of sequence C is due to the existence of low-lying semi compact conformations, not present for thermodynamically stable sequences. The consequences of these low-lying states for the folding dynamics will be investigated in what follows.

### 3.2 Thermodynamic stability: compact state spectrum versus transition width

In order to answer the first question in item (i) in the introductory section, we want to compare the compact-state-spectrum estimation of the thermodynamic stability, in terms of the folding temperature  $T_f$  and the glass-transition temperature  $T_g$  [18, 20], to the thermodynamic stability estimated with the method of section 3.1.

#### 3.2.1 Compact-state-spectrum results

We first review the results of Goldstein *et al.* [18], and Bryngelson *et al.* [20], who estimated the folding temperature  $T_f$  and the glass temperature  $T_g$  in terms of simple spectral quantities. These authors derived their criteria from the complete energy spectrum, dividing phase space into two components: on the one hand, the native state with a nearly zero entropy and, on the other hand, uncorrelated “liquid-like” states at higher energy with a large entropy. If  $\Delta$  denotes the average

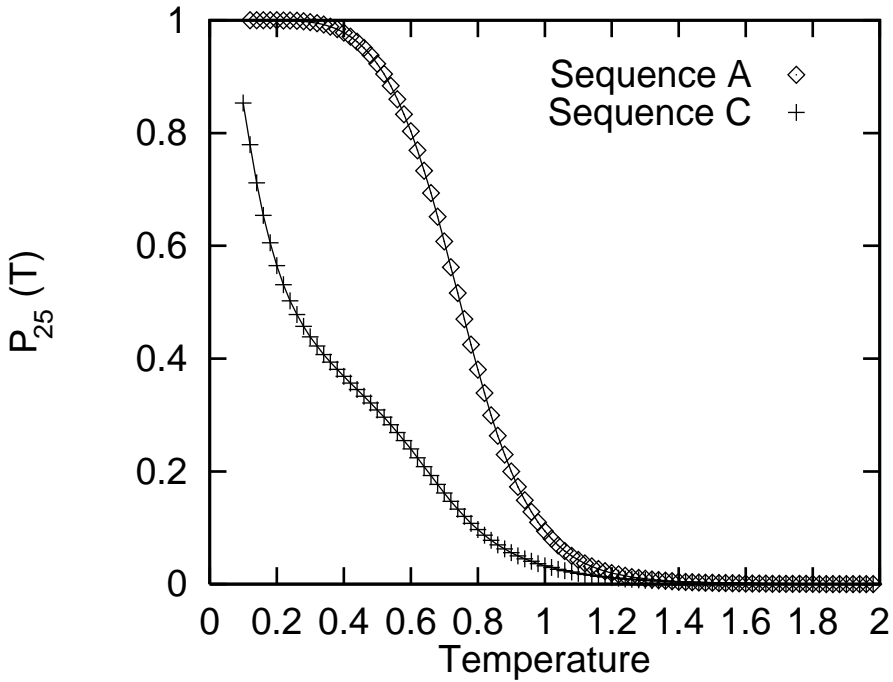


Figure 2: Probability  $\mathcal{P}_{25}(T)$  to be in any state having more than 25 native contacts as a function of temperature for the thermodynamically stable sequence A and the thermodynamically unstable sequence C.

energy difference between the native and the liquid-like states, and  $\Gamma$  is the width in energy of the liquid-like states, it is shown in [18, 20] that the ratio  $T_f/T_g$  is maximal if  $\Delta/\Gamma$  is maximal. In other words, the ratio  $\Delta/\Gamma$  should measure how “protein-like” a sequence is. We take here as a working hypothesis the application of the results in [18, 20] to our lattice model including the compact states only. In order to test the hypothesis, we calculate  $\Delta$  and  $\Gamma$  from the compact-state spectra, the compact states being conformations exactly filling the  $3 \times 3 \times 3$  cube, and the compact-state spectrum of a given sequence being the set of energies of all compact conformations. More precisely,

$$\Delta = \frac{1}{N_C} \sum_{\alpha>0} (E_\alpha - E_0) \quad (7)$$

$$\Gamma^2 = \frac{1}{N_C} \sum_{\alpha>0} E_\alpha^2 - \left( \frac{1}{N_C} \sum_{\alpha>0} E_\alpha \right)^2, \quad (8)$$

where the  $E_\alpha$  ( $\alpha > 0$ ) denote the energies of the excited compact conformations,  $E_0$  is the lowest compact state energy, and  $N_C$  is the number of excited compact conformations.

### 3.2.2 Thermodynamic stability versus $\Delta/\Gamma$

As far as the Monte Carlo results are concerned, we estimate the thermal stability of a sequence by the width of the transition in  $\mathcal{P}_{25}(T)$  versus  $T$ , as shown in Fig. 2. More precisely, we calculate the

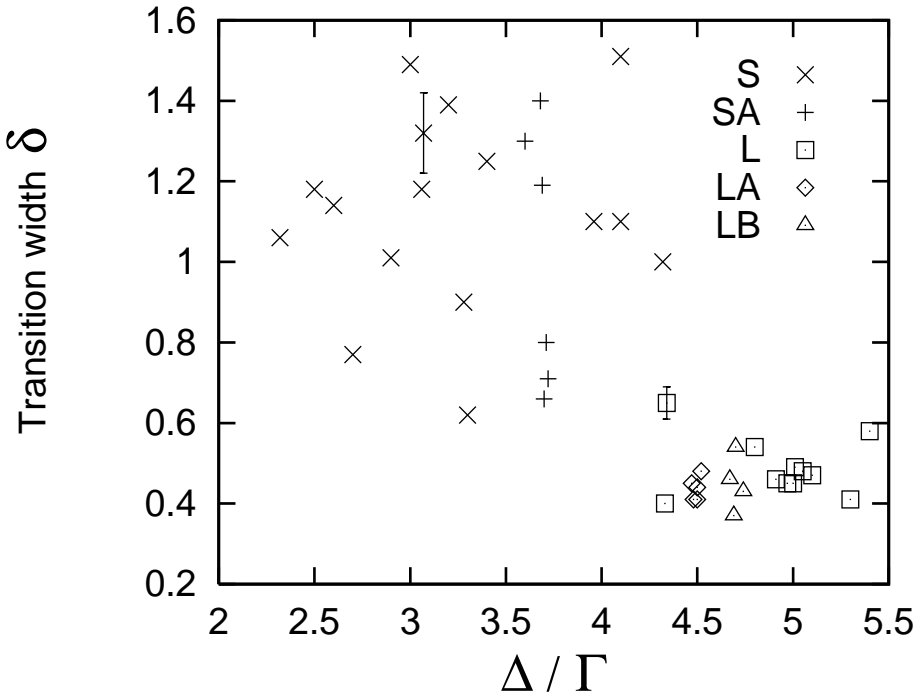


Figure 3: Transition width  $\delta$  from the Monte-Carlo simulations versus  $\Delta/\Gamma$  obtained from the compact-state spectrum. As explained in the text, the different sets and sub-sets of sequences are denoted by different symbols. Typical error bars in the estimation of  $\delta$  are shown. The larger error bars for large  $\delta$  originate from the increase of glassiness as  $\delta$  increases.

dimensionless transition width as

$$\delta = 2 \left( \frac{T(0.1) - T(0.8)}{T(0.1) + T(0.8)} \right), \quad (9)$$

where  $T(x)$  is the temperature for which the probability is  $x$  to find the heteropolymer in a state with 25 or more native contacts. [This is the inverse function of  $\mathcal{P}_{25}(T)$  as plotted on Fig. 2]. We have plotted in Fig. 3 the width  $\delta$  of the transition as a function of  $\Delta/\Gamma$  defined by (7) and (8). We have separated the sequences into a set “L(arge)” of sequences with large values of  $\Delta/\Gamma$  and a set “S(mall)” with small values of this ratio. (For further consideration, we have extracted from the “L” set two subsets “LA” and “LB” with a fixed  $\Delta/\Gamma$  ratio, of order 4.5 and 4.7 respectively. Also, the set “SA” has been extracted from the “S” set, with a  $\Delta/\Gamma$  ratio of order 3.7.) It is clear in Fig. 3 that in spite of some scatter, the “L”, “LA” and “LB” sets, with a high  $\Delta/\Gamma$  ratio (larger than 4.3) correspond to thermodynamically stable sequences, with a narrow transition to the native structure (*i.e.*, a small  $\delta$  value), whereas the transition to the native structure for the sequences belonging to the “S” and “SA” sets ( $\Delta/\Gamma < 4.3$ ) is rather broad. This shows that “protein-like” sequences (at least as far as thermodynamics is concerned) correspond to sequences with a large  $\Delta/\Gamma$  ratio, *i.e.* sequences with a low-energy native state compared to the energy width of the distribution of compact states.

One can also ask how the transition width  $\delta$  correlates with  $\Delta$  alone, independent of  $\Gamma$ . It turns

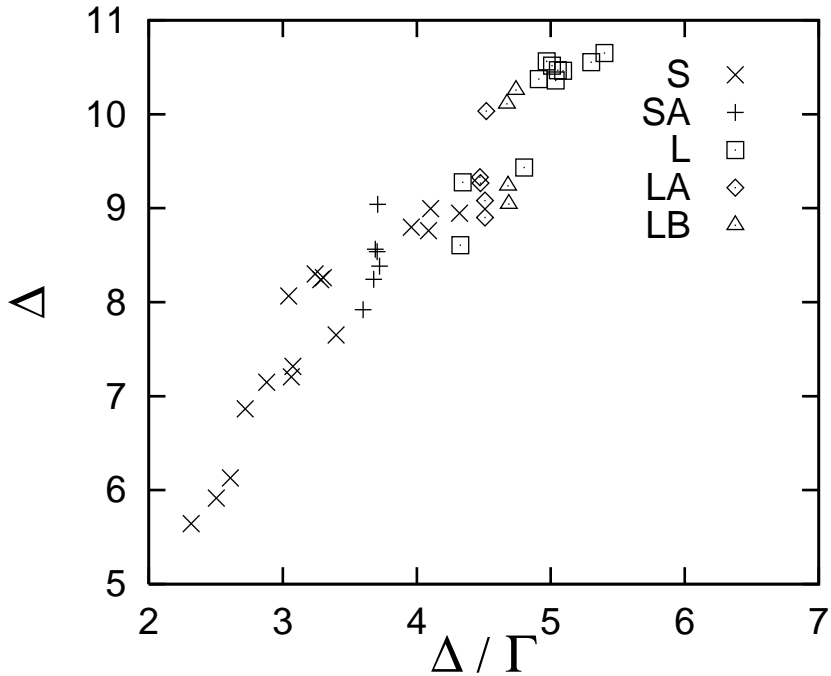


Figure 4:  $\Delta$  versus  $\Delta/\Gamma$  for our 45 sequences selection. The symbols are the same as in Fig. 3.

out that  $\Delta/\Gamma$  is almost a monotonically increasing function of  $\Delta$ , as shown in Fig. 4,  $\Gamma$  being nearly constant at  $\Gamma \simeq 2$ , and therefore  $\Delta$  alone is also a good predictor of thermodynamic stability.

### 3.3 Thermodynamic stability versus designability

The designability of a given structure is measured in terms of the number  $N_S$  of sequences that have this structure as their nondegenerate ground state, and, as proposed in [13], the sequences corresponding to highly designable structures should be “protein-like”. Interestingly, the highly designable structures show regular helix-like and  $\beta$ -sheet-like patterns [13], quite reminiscent of the regular patterns in real proteins. Moreover, since these highly designable structures have on average a large gap to their first compact excited state [13], they are likely to be thermodynamically stable. More specifically, the average gap in the compact state spectrum suddenly jumps from a low value to a high value as  $N_S$  increases above  $N_S \sim 1400$ . It is thus of interest to relate the thermodynamic stability of sequences, measured in terms of  $\delta$  in equation (9), to the degree of designability of their native state structure measured by  $N_S$ . We will reach the conclusion that  $\Delta/\Gamma$  is a better predictor of thermodynamic stability than designability. Qualitatively, this could be anticipated since high designability of a structure still allows for very different behaviors of the sequences which design that structure.

The correlation between the transition width  $\delta$  of the various sequences analyzed here, and the number  $N_S$  of sequences that design their native structures is plotted in Fig. 5. Clearly, the sequences whose ground states are highly designable structures are likely to be thermodynamically stable. However, we observe that several sequences belonging to the sets “S” and “SA” of thermody-

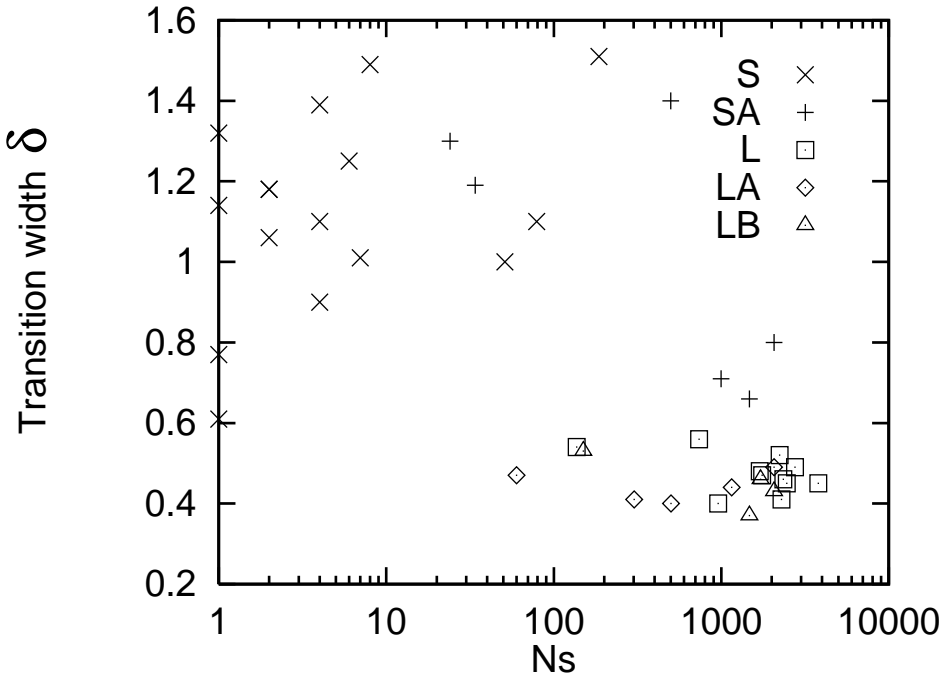


Figure 5: Transition width  $\delta$  versus the number  $N_S$  of sequences that design a given structure. Crosses denote sequences with a small  $\Delta/\Gamma$  ratio and squares, diamonds and triangles sequences with a large  $\Delta/\Gamma$ . Some sequences in the SA sub-set with  $\Delta/\Gamma \simeq 3.7$  can have a large designability in spite of being thermodynamically unstable.

namically unstable sequences have a relatively high designability  $N_s$ . These sequences, despite high designability, have a small value of  $\Delta/\Gamma$ . Such sequences are expected to emerge due to the fact that, even for a structure with large  $N_S$ , the ratio  $\Delta/\Gamma$  is not necessarily large for all sequences having that structure as a ground state [21]. In other words, it is possible to find atypical sequences with a low value of  $\Delta/\Gamma$  even for structures with a large  $N_S$ . For instance, using the compact-state spectra, we have plotted in Fig. 6 the distribution of  $\Delta/\Gamma$  for the top structure (this is the structure with the maximal  $N_S = 3794$ ) and a structure with  $N_S = 300$ . On average the sequences corresponding to the structure with  $N_S = 3794$  have larger  $\Delta/\Gamma$  than the sequences corresponding to the structure with  $N_S = 300$ . However, the tail of the distribution for the  $N_S = 3794$  structure still extends to very small  $\Delta/\Gamma$ . In summary, large  $\Delta/\Gamma$  ratio is a good predictor that a sequence will be thermodynamically stable. A high designability  $N_S$  for a structure is consistent with, but does not guarantee, large  $\Delta/\Gamma$  and hence thermodynamic stability of its associated sequences.

Finally, we would like to comment on the results of Vendruscolo *et al.* [14]. These authors also carried out an analysis of the relation between thermodynamic stability, calculated with all the configurations including the open ones, and the number of sequences  $N_S$  that design a given structure. The authors analyzed the two dimensional case of the present model with 16 monomer chains and exactly enumerated not only all the possible compact but also all the possible open state conformations. They found first, in agreement with Li *et al.* [13], a broad distribution of  $N_S$ .

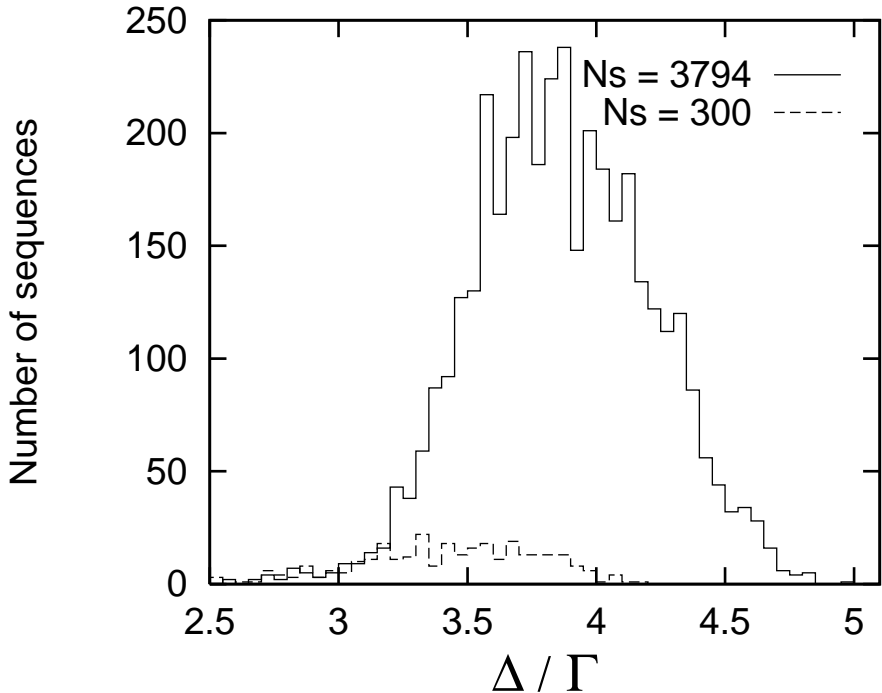


Figure 6: Distribution of  $\Delta/\Gamma$  for the top structure (structure with the maximal  $N_S = 3794$ , solid line) and a structure with  $N_S = 300$  (dashed line). Each bin has a width of 0.05 in  $\Delta/\Gamma$  and the quantity on the  $y$  axis measures how many sequences fall in each bin.

However, they showed that the thermodynamic stability is flat as a function of  $N_S$ , in contradiction with our present results, and also in contradiction with unpublished data [22] where the gap in the compact state spectrum in two dimensions was shown to increase as a function of  $N_S$ . In our opinion, this discrepancy is due to the fact that in [14] the overall compactness energy  $E_C$  in the inter-residue interactions was set to zero, thereby weighting open state configurations too strongly with respect to compact states. We expect that a larger  $E_C$  would have led to an  $N_S$ -dependence of the thermodynamic stability in Ref. [14].

### 3.4 Conclusions on the thermodynamics

This section was devoted to the analysis of the thermodynamics of several sequences, selected from highly and poorly designable sequences, and with large and small values of  $\Delta/\Gamma$ . The known compact state spectra allow for the calculation of the ratio  $\Delta/\Gamma$ , which is thought to be proportional to the ratio of the folding temperature to the glass temperature [18, 20], and thus predicts to what extent a given sequence is thermodynamically “protein-like”. The Monte-Carlo data calculated with open and partially open states also allowed us to characterize the thermodynamic stability of a given sequence, in terms of the width  $\delta$  of its folding transition. We have shown that these two quantities,  $\delta$  and  $\Delta/\Gamma$ , are well correlated, signaling the validity of the compact-state-spectrum analysis. We have also shown that stability with respect to mutations (measured in terms of designability) is not directly equivalent to thermal stability.

Finally, it is worth noting that we eliminated three sequences with partially open ground states. These sequences had a very low  $\Delta/\Gamma$  ratio (2.17, 2.18, 2.52) [this ratio has been calculated with the ground state energy  $E_0$  being the lowest compact state energy]. By contrast, none of the simulated sequences with a high or moderate  $\Delta/\Gamma$  ratio were found to have a partially open ground state. This suggests that the ground state conformation of some of the remaining sequences with a small  $\Delta/\Gamma$  ratio may not be compact. However, since these sequences are among the most unstable ones, our calculation of the transition widths as far as “protein-like” sequences are concerned is unaffected.

## 4 Folding simulations

Besides thermodynamic stability and stability with respect to mutations of the amino-acid code, the native state of a “protein-like” sequence should be dynamically accessible. Clearly, the dynamics of all the sequences, including the thermodynamically stable ones, becomes glassy at low temperatures in our model since all the inter-residue interactions are attractive. As the temperature is lowered, the average folding time (the average time required to first reach the native states, starting from a stretched conformation) will first decrease and then, below a certain temperature, will start to increase drastically, presumably scaling like  $\ln(\langle\tau_f\rangle) \sim 1/T$ . Conversely, as we have already seen, the native state occupancy increases as the temperature is decreased. Since we want to investigate the balance between thermodynamic stability and dynamical accessibility of the native state, we chose to examine the dynamics at the temperature  $T_f$  such that the native state occupancy is fixed at some predetermined  $\mathcal{P}_f$ . The question is then: do the sequences with a large  $\Delta/\Gamma$  ratio, thermodynamic stability, and mutational stability also fold fast at  $T_f$ ?

In order to examine this question, we measured the average folding time, namely the average time  $\langle\tau_f\rangle$  necessary for the heteropolymer to first reach any of the native states (with 25 ground state contacts, out of 28), starting from a stretched conformation. Because in our model all interaction energies are attractive, and individual non-native contacts may be as strong as native contacts, the folding dynamics is very slow compared to other models. For this reason, we simulated folding of the heteropolymers at the temperature  $T_f$  such that the average occupancy of the native states is only  $\mathcal{P}_f = 10\%$ . Compared to other works where models with a faster folding time were investigated, this occupancy of the native states is quite small. For instance, Abkevich *et al.* [23] could fold a few sequences at a temperature for which the average similarity with ground state was up to 95%. Their slowest average folding time was then of the order of  $2 \times 10^8$  MCS, which is one order of magnitude smaller than the fastest folding time in our simulations (given that 1 BKL unit = 27 MCS). However, models with faster folding times generally require unrealistic assumptions such as artificially lower energy for individual native contacts compared to the non-native ones. Even though we could not go systematically to lower temperatures, the effect of lowering the temperature was examined for a few sequences.

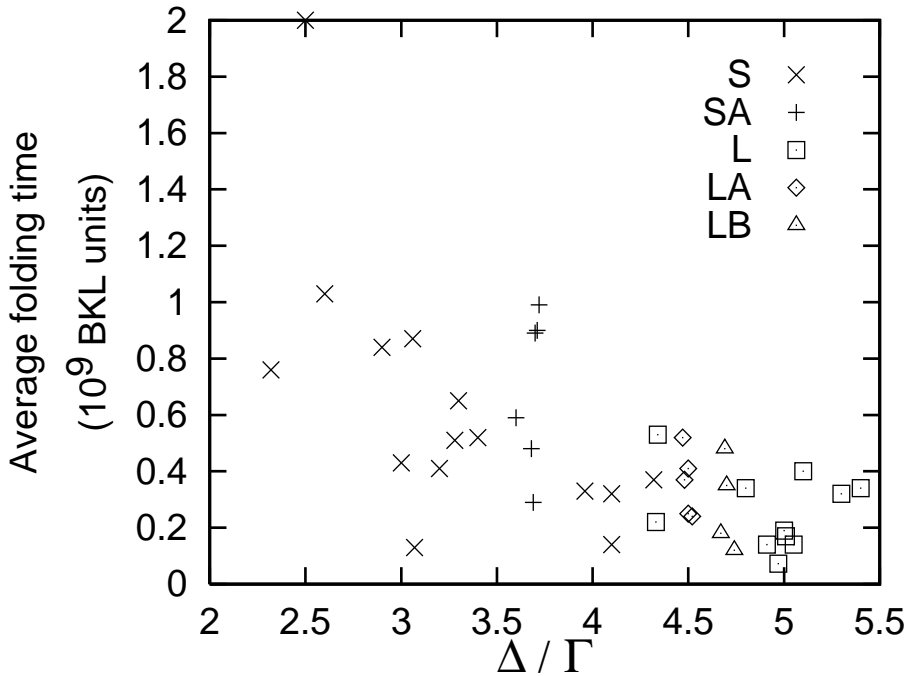


Figure 7: Average folding times (in BKL units) versus  $\Delta/\Gamma$ , with the same symbols as Figs. 3, 4, and 5. A very slow folding sequence (hereafter denoted by “W(orst)”) has not been shown. It belongs to the set “S”, has  $\Delta/\Gamma = 2.7$ , and an average folding time of  $4.3 \times 10^9$  BKL units.

#### 4.1 Average folding times

One folding simulation consists in starting from a stretched heteropolymer, and running the dynamics until one of the native states is first reached. The time required is the folding time, which should then be averaged over several folding simulations. In practice, we have averaged the folding time over 20 folding simulations. For each sequence, the temperature is fixed at  $T_f$  (at this temperature, the native-states occupancy is  $\mathcal{P}_f = 10\%$ ). The average folding times are plotted in Fig. 7 as a function of  $\Delta/\Gamma$ . The relative error in the average folding time can be estimated by noticing that the mean value of the folding time distribution is of the order of the standard deviation (we indeed calculated the full folding time distribution for a few sequences). The relative error in the estimation of the average folding time is then of the order of the inverse square root of the number of folding simulations, namely, in our case of  $1/\sqrt{20} \simeq 0.2$ . This precision is sufficient for the purpose of our discussion.

We observe in Fig. 7 that sequences with a large  $\Delta/\Gamma$  ratio fold fast. We thus conclude, in response to question (iii) in the introductory section, that folding dynamics does not add any constraint in the selection of “protein-like” sequences: once a structure is stable against mutations and thermodynamically stable (namely, a sequence with a large  $\Delta/\Gamma$  ratio and a large  $N_S$ ), it will be a fast folder.

A quite striking result visible in Fig. 7, is that sequences with a low  $\Delta/\Gamma$  ratio (belonging to the “S” and “SA” sets of thermodynamically unstable sequences), may also fold fast, at least as fast as

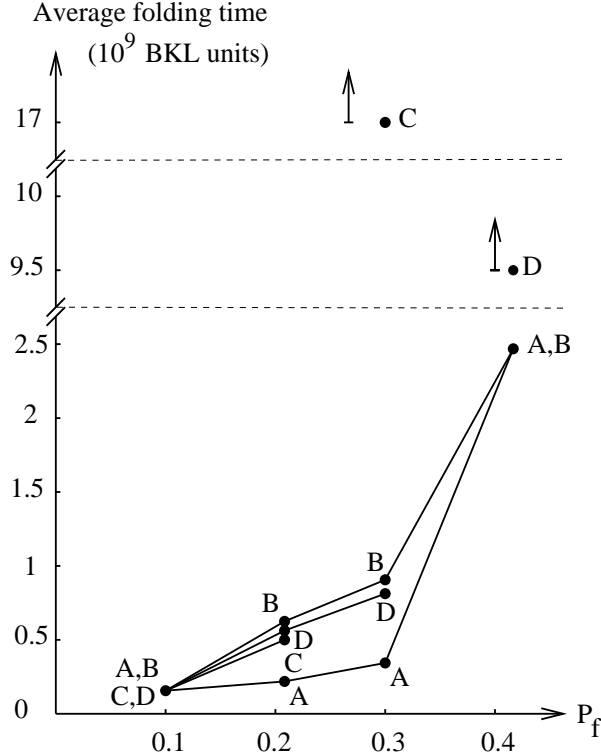


Figure 8: Folding time of the four sequences A, B, C and D for various native-states occupancies. The value of  $\Delta/\Gamma$  for the four sequences A, B, C and D is respectively 5.05, 4.91, 4.1 and 3.07. The sequences A and B are thermodynamically stable, and C and D are thermodynamically unstable. The two arrows indicate that the corresponding folding times are a lower bound.

some of the sequences belonging to the “L”, “LA” or “LB” sets. However, at lower temperatures and hence larger native-states occupancy, we find a stronger correlation between low  $\Delta/\Gamma$  ratio and slow folding.

In order to go to lower temperatures, we selected four sequences (denoted by A, B, C, and D; A and C being the same sequences as in Fig. 2), with the same fast folding time,  $0.14 \times 10^9$  MCS, at  $T_f$ , i.e. with a 10% occupancy of conformations with 25 or more native contacts. We folded these sequences again at temperatures corresponding to larger native-states occupancy. The sequences A and B belong to the set “L” of thermodynamically stable sequences, and the sequences C and D belong to the set “S” of thermodynamically unstable sequences. As the native-states occupancy is increased, we observe in Fig. 8 that the folding times of the two thermodynamically unstable sequences, C and D, clearly become much larger than the folding times of the two thermodynamically stable sequences, A and B. Regarding the results of our study at a fixed native-states occupancy of 10% (see Fig. 7), this suggests that, as the native-states occupancy increases, the average folding times of the sequences with small  $\Delta/\Gamma$  ratio will increase much more rapidly than the folding time of the sequences with large  $\Delta/\Gamma$  ratio.

The conclusion regarding the variations of the average folding times as a function of the native-states occupancy is similar to the one reached by Abkevich *et al.* [23], who proposed that the gap  $\Delta$  in the compact-state spectrum correlates with the average folding time calculated for large native-states occupancy.

## 4.2 Slow versus fast folding

Despite the complexity of protein energy landscapes, several authors have proposed simple effective descriptions of these landscapes. For instance, the role of traps (or folding intermediates) in the folding process was underlined by several authors, for instance by Bryngelson and Wolynes [24] and by Klimov and Thirumalai [6]. A scenario was proposed by Bryngelson *et al.* [25] in which there exists a “folding pathway” to the native state: in a first step, the protein collapses via many possible paths in phase space, and, in a second step, folds to the native structure via a small number of possible paths. Abkevich *et al.* found evidence for a nucleation process in a lattice model study [26]. The aim of the present section is to see if there exists any simple scenario in our H-P model.

Among all the sequences analyzed here at a  $\mathcal{P}_f = 10\%$  occupancy of native states, one sequence has an anomalously long folding time, approximatively  $4 \times 10^9$  MCS. This sequence belongs to the set of thermodynamically unstable sequences ( $\Delta/\Gamma = 2.7$  and  $\delta = 0.77$ ). Since this sequence has the longest folding time among our sequence selection, we will denote this sequence by “W(orst)”. We will compare this very slow folding sequence to a fast folding “protein-like” sequence (sequence A in Fig. 8), and also to a sequence which is thermodynamically unstable but folds fast at a native-states occupancy of  $\mathcal{P}_f = 10\%$  (sequence C in Fig. 8).

### 4.2.1 Number of low-energy conformations

In order to obtain more information on low-energy traps, we carry out the following simulation. We start from a stretched conformation and let the dynamics evolve until a conformation is first reached whose energy above the ground state  $\Delta E = E - E_0$  is smaller than a given  $\Delta E_{\text{hit}}$ . We refer to the result of a single such simulation as a “hit”. The contact matrix of this conformation is then recorded. (The contact matrix encodes a compact or nearly compact structure in a unique way. Its matrix elements  $\mathcal{C}_{i,j}$ , with  $i, j = 1, \dots, 27$ , labeling the monomers along the chain, are equal to unity if the monomers  $i$  and  $j$  are in contact, and zero otherwise.) We repeat this simulation  $N$  times ( $N = 1500$  in practice). We have chosen a small  $\Delta E_{\text{hit}} = 0.5$ , but similar conclusions were obtained with  $\Delta E_{\text{hit}} = 1$ . We finally examine the different structures encoded in the set of contact matrices  $\mathcal{C}^{(1)}, \dots, \mathcal{C}^{(N)}$  of the  $N$  “hits”.

We analyzed three sequences: sequence A (a “protein-like” sequence), sequence C (fast folding at  $\mathcal{P}_f = 10\%$  occupation of native states, but thermodynamically unstable), and the very slow folding sequence W.

| Density of hits (%) | $d_{GS}$ | Density of hits (%) | $d_{GS}$ |
|---------------------|----------|---------------------|----------|
| 21.0                | 28       | 6.0                 | 38       |
| 17.7                | 32       | 5.4                 | 40       |
| 10.9                | 30       | 4.7                 | 38       |
| 10.7                | 38       | 3.9                 | 34       |
| 8.7                 | 26       | 2.1 (GS)            | 0 (GS)   |
| 7.9                 | 34       | 1.2                 | 40       |

Table 1: The twelve structures obtained for sequence C. The energy of these structures is  $\Delta E = 0.3$  (except for the ground state that has  $\Delta E = 0$ ). The first column is the density of hits (probability that a given structure is hit) and the second column is the Hamming distance to the ground state. The ground state is indicated in the table.

We first study the number of different structures for the sequences A, C, and W. It turns out that the “protein-like” sequence A, no states other than the ground state were found with an energy  $\Delta E < \Delta E_{\text{hit}} = 0.5$ . As far as the two other sequences C and W are concerned, we found 12 different structures for sequence C and 125 for sequence W. The list of these structures obtained is shown in Table 1 for sequence C and Table 2 for sequence W. The Hamming distance to the ground state in the second column of these tables is

$$d(\mathcal{C}, \mathcal{C}^{(GS)}) = \sum_{i=1}^{27} \sum_{j=i+3}^{27} |\mathcal{C}_{i,j} - \mathcal{C}_{i,j}^{(GS)}|, \quad (10)$$

with  $\mathcal{C}$  the contact matrix of a given hit and  $\mathcal{C}^{(GS)}$  the contact matrix of the ground state structure. The contact matrices being symmetric, the summation in (10) is restricted to the matrix elements  $i \leq j$ . The matrix elements  $j = i + 1$  have been discarded since they correspond to covalent bonds; the matrix elements  $j = i + 2$  have also been discarded since no contact can be made between these monomers.

We conclude that, going from the “protein-like” sequence A to sequence C and to the very slow folder W, one has a spectacular proliferation of different low-energy conformations that can be hit starting from a stretched conformation. It is also worth remarking that the ground state structure is not the most likely to be hit for either sequence C or W.

In order to determine if any structures with energy  $\Delta E < \Delta E_{\text{hit}} = 0.5$  have been missed, we first notice that for sequence C, the most unlikely hit has been reached 18 times out of  $N = 1500$  simulations (the density of hits for this structure is 1.2%, as shown in Table 1). This number is much larger than unity, indicating that all structures of comparable or greater probability have been found. For sequence W, the most unlikely hits have been reached only once out of the  $N = 1500$  simulations, strongly suggesting that some of the low-energy structures have not been found. In order to estimate

| Density of hits (%) | $d_{GS}$ |
|---------------------|----------|---------------------|----------|---------------------|----------|---------------------|----------|
| 4.7                 | 46       | 1.0                 | 42       | * 0.5               | 32       | * 0.3               | 42       |
| 4.5                 | 44       | * 1.0               | 42       | * 0.5               | 40       | * 0.3               | 48       |
| 3.4                 | 48       | 0.9                 | 46       | 0.5                 | 42       | * 0.3               | 50       |
| 3.3                 | 44       | * 0.9               | 44       | 0.5                 | 44       | * 0.3               | 44       |
| 3.3                 | 46       | * 0.9               | 34       | * 0.5               | 12       | * 0.3 (GS)          | 0 (GS)   |
| 3.1                 | 46       | 0.9                 | 42       | * 0.5               | 50       | 0.3                 | 38       |
| 2.1                 | 42       | 0.9                 | 44       | * 0.5               | 42       | * 0.3               | 38       |
| 2.1                 | 42       | * 0.9               | 40       | 0.5                 | 46       | * 0.2               | 40       |
| 2.1                 | 48       | * 0.9               | 46       | 0.5                 | 46       | * 0.2               | 34       |
| * 2.0               | 46       | * 0.9               | 38       | 0.5                 | 44       | 0.2                 | 38       |
| 1.9                 | 42       | * 0.9               | 50       | 0.5                 | 44       | * 0.2               | 40       |
| 1.7                 | 40       | * 0.8               | 38       | * 0.4               | 42       | * 0.2               | 44       |
| * 1.7               | 46       | * 0.8               | 44       | * 0.4               | 42       | 0.2                 | 42       |
| 1.6                 | 40       | * 0.8               | 42       | * 0.4               | 36       | * 0.2               | 42       |
| 1.5                 | 46       | * 0.8               | 32       | * 0.4               | 36       | * 0.1               | 48       |
| * 1.5               | 40       | * 0.8               | 42       | * 0.4               | 46       | * 0.1               | 46       |
| * 1.4               | 38       | 0.7                 | 52       | * 0.4               | 44       | 0.1                 | 36       |
| * 1.4               | 44       | * 0.7               | 40       | * 0.4               | 38       | * 0.1               | 38       |
| * 1.3               | 38       | 0.7                 | 40       | 0.4                 | 44       | * 0.1               | 26       |
| * 1.3               | 38       | * 0.7               | 30       | * 0.4               | 38       | * 0.1               | 44       |
| 1.3                 | 48       | * 0.7               | 46       | * 0.3               | 40       | 0.1                 | 38       |
| 1.3                 | 40       | * 0.7               | 50       | * 0.3               | 50       | * 0.1               | 40       |
| * 1.2               | 46       | * 0.7               | 46       | 0.3                 | 36       | * 0.1               | 44       |
| 1.2                 | 42       | 0.6                 | 48       | * 0.3               | 42       | * 0.1               | 36       |
| * 1.2               | 38       | 0.6                 | 46       | * 0.3               | 46       | * 0.1               | 50       |
| 1.1                 | 46       | 0.6                 | 40       | * 0.3               | 40       | * 0.1               | 36       |
| * 1.1               | 32       | * 0.6               | 46       | * 0.3               | 50       | * 0.1               | 50       |
| * 1.1               | 32       | 0.6                 | 42       | * 0.3               | 42       | * 0.1               | 46       |
| 1.1                 | 44       | 0.6                 | 42       | * 0.3               | 42       | 0.1                 | 40       |
| * 1.1               | 42       | * 0.6               | 34       | * 0.3               | 38       | * 0.1               | 52       |
| * 1.0               | 40       | 0.6                 | 44       | 0.3                 | 48       | * 0.1               | 50       |
|                     |          |                     |          |                     |          | * 0.1               | 46       |

Table 2: The 125 structures obtained for sequence W. The energy of all these structures is  $\Delta E = 0.3$ , except for the ground state that has  $\Delta E = 0$ , and all states are highly compact, with a number of contacts  $\geq 26$  out of 28 possible. The first column is the density of hits (probability that a given structure is hit first) and the second column is the Hamming distance to the native state. The ground state is indicated in the table. The symbol \* denotes a compact structure.

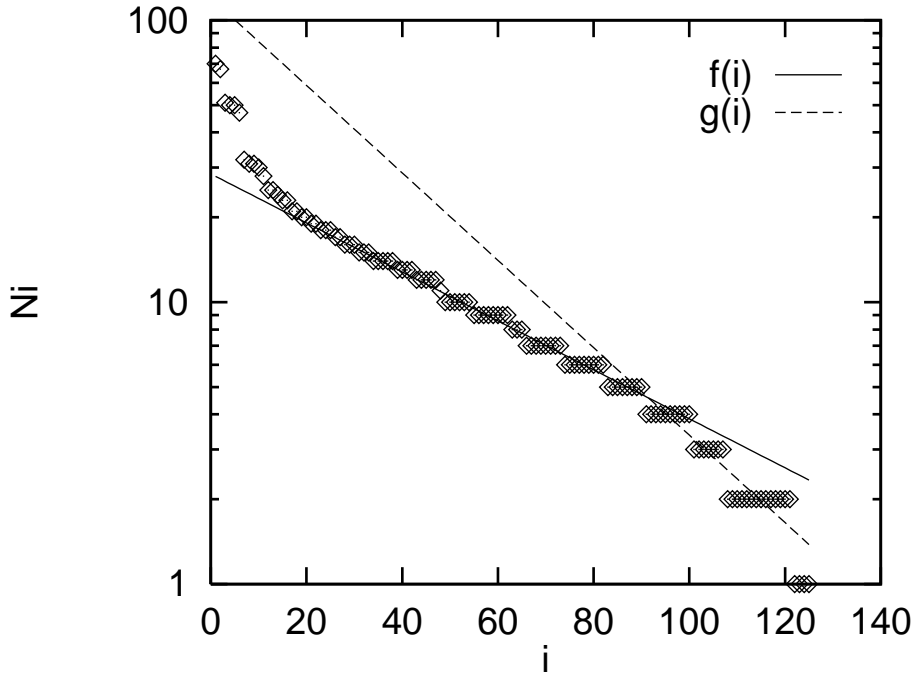


Figure 9: Variations of the number of hits  $i$  versus their rank  $i$ .

the number of missed structures for sequence W, we have plotted in Fig. 9 the number of times  $N_i$  a structure has been reached, ordered in decreasing order. The tails have been fitted to an exponential decay  $f(i) = 28.5 \exp(-i/50)$  if  $i < 90$  and  $g(i) = 120 \exp(-x/28)$  if  $i > 90$ . An estimate of the error in the total number of structures can be obtained by extrapolating  $g(i)$  and solving for  $g(i) = 1$ , which leads to  $i = 134$ , compared to the 125 different structures obtained. This indicates that of order 10 structures with  $\Delta E < \Delta E_{\text{hit}} = 0.5$  were not reached in the  $N = 1500$  simulations.

We have also compared the states hit in the folding simulation to the complete set of compact low-energy states with an energy  $\Delta E < \Delta E_{\text{hit}} = 0.5$  (known from the compact-state enumeration [13]). In the case of sequence C, we found that all 12 low-energy states in Table 1 are indeed compact, and correspond exactly to all the compact states with an energy  $\Delta E < \Delta E_{\text{hit}} = 0.5$ . For sequence W, we found 85 compact structures with an energy  $\Delta E < \Delta E_{\text{hit}} = 0.5$ , a number considerably smaller than the 125 structures in Table 2, which include partially open structures as well. Moreover, five of the 85 compact-state structures were not hit in our simulations. It is very plausible that these five low-energy compact structures were missed because of poor statistics for the most unlikely hits; this is consistent with the earlier statistical estimate of a total of 10 missed structures.

The comparison between the low-energy compact structures and the hit simulations shows that, for the average folding sequence C, the full low-energy phase space is dynamically accessible, though some of these low-energy conformations are more likely to be hit (see Table 2). The proliferation of different low-energy conformations in the case of the slow folding sequence W closely matches the large number of low-energy compact conformations. This is natural because the low energy cut-off  $\Delta E_{\text{hit}} = 0.5$  restricts “hits” to compact or very-close-to compact states.

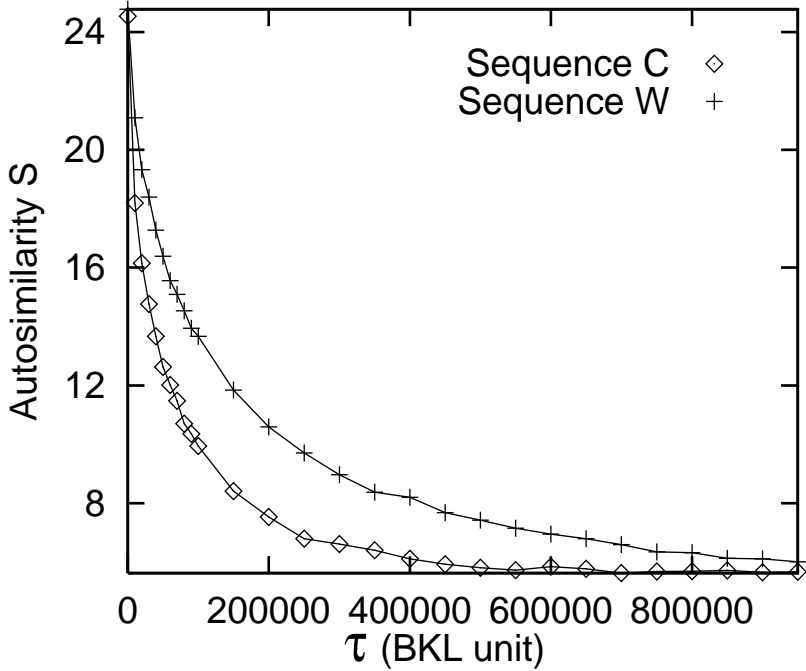


Figure 10: Evolution of the similarity  $S(t_0, \tau)$  between the conformation at times  $t_0$  and  $t_0 + \tau$ .

#### 4.2.2 “Trapping” time in the low energy conformations

We now turn to the question of how long the protein remains in the first states reached with an energy  $\Delta E < \Delta E_{\text{hit}}$ . In particular, we would like to compare the magnitudes of the “trapping times” in these low-energy states. To do so, we start from a stretched conformation and let the dynamics evolve until a state with energy  $\Delta E < \Delta E_{\text{hit}}$  is first met at time  $t_0$ . We then calculate the similarity  $S(t_0, \tau)$  between the conformation at time  $t_0$  and at a later time  $t_0 + \tau$ . This quantity is then averaged over  $N = 1500$  complete simulations. The results are plotted in Fig. 10 for the sequences C and W, for  $\Delta E_{\text{hit}} = 0.5$ . As is visible in this figure, the typical “trapping time” in a conformation with an energy  $\Delta E < \Delta E_{\text{hit}}$  differs by only a factor of 2 or 3 between the sequences C and W, compared to a factor of 30 difference in folding times. This observation further confirms that the slow folding of sequence W does not originate from the trapping in a few “valleys” in phase space with a very long trapping time. On the contrary, the trapping time of the average folder C and the very slow folder W is of the same order of magnitude and slow folding seems to originate primarily from the profusion of low-energy conformations for sequence W.

## 5 Conclusion

Let us now summarize our answers to the three questions presented in the introduction.

- (i) We have investigated the relation between compact-state-spectrum predictions, namely the  $\Delta/\Gamma$  criterion, Eqs. (7) and (8), and thermodynamic stability, determined from Monte-Carlo

simulations where all the states (not only the compact ones) are taken into account. We find that for high  $\Delta/\Gamma$  the predictions of the compact-state-spectrum analysis are in good agreement with the Monte-Carlo simulations. Namely, sequences that have a high  $\Delta/\Gamma$  ratio also have a sharp transition to the native state conformations (“thermodynamically stable”). For sequences with low and intermediate  $\Delta/\Gamma$  ratio, the transition widths vary considerably and are generally broader. This suggests that low energy open configurations can be important in determining  $\delta$  in this case. We find that designability (defined as the number of sequences that have a given structure as their nondegenerate ground state) is not in one-to-one correspondence with thermodynamic stability. Some sequences with highly designable ground states are thermodynamically unstable. However, we did find that sequences with highly designable ground states have *on average* a large  $\Delta/\Gamma$  ratio, and that sequences with poorly designable ground states have *on average* a small  $\Delta/\Gamma$  ratio.

- (ii) The folding simulations have shown that sequences with a large  $\Delta/\Gamma$  ratio fold fast. Sequences with a low  $\Delta/\Gamma$  ratio, and therefore sequences which are thermodynamically unstable, may fold slow or fast at the relatively high temperatures that we investigated. At these temperatures the protein spends only 10% of the time near its ground-state configuration. We have argued, with several examples, that at lower temperatures the thermodynamically unstable sequences are likely to become slow folders whereas the stable ones are likely to continue to fold fast.
- (iii) To be “protein-like” a sequence must first be thermodynamically stable, which follows if it has a large  $\Delta/\Gamma$  ratio. Second, the sequence must be mutationally stable, which follows if it has a highly designable ground state. We find that the third requirement to be “protein-like”, namely fast folding, does not introduce additional constraints on sequence selection. Once a sequence has been designed to be thermodynamically stable (large  $\Delta/\Gamma$ ) and stable against mutations (large  $N_S$ ) its folding dynamics is fast.

We have also explored the reason for the slow folding of a sequence with an anomalously large average folding time. We found that the “trapping time” in a given low energy state is of the same order of magnitude for both fast and slow sequences, and cannot explain the large differences in the average folding times. Instead, we have shown that the slow folder visits a large number of different low-energy states, whereas only a few low-energy states are visited by the fast folder. This suggests that slow folding dynamics originates from a large number of low energy conformations.

Finally, we make a few remarks to illustrate the magnitude of structure and sequence selection. We started from a set of  $2^{27}$  sequences, only 4.75% (approximately 6,000,000) of these having a nondegenerate compact ground-state [13] structure. The total number of possible compact structures is 51,704 [13]. Among all these structures, only 60 are highly designable (estimated from the jump of

the average compact-state-spectrum gap as  $N_S$  increases above  $\simeq 1400$  [13]). The 60 highly designable structures are designed by a total of 128,320 sequences, only 15% of which have  $\Delta/\Gamma > 4.3$  and are thus expected to be “protein-like” folders. In summary, only about 0.01% of the initial  $2^{27}$  sequences satisfy all the requirements for “protein-like” behavior.

Acknowledgements: The authors acknowledge useful discussions with C. Denniston and G. Parisi. Part of this work was carried out when R.M. was a post-doctoral fellow at the International School for Advanced Studies (SISSA) at Trieste.

## References

- [1] C.B. Anfissen, *Science* **181**, 223 (1973).
- [2] H.S. Chan and K.A. Dill, *J. Chem. Phys.* **99**, 2116 (1993); *ibid*, **100**, 9238 (1994).
- [3] E. Shakhnovich, G. Farztdinov, A.M. Gutin, and M. Karplus, *Phys. Rev. Lett.* **67**, 1665 (1991).
- [4] A. Sali, E. Shakhnovich, and M. Karplus, *Nature* **369**, 248 (1994); *J. Mol. Biol.* **235**, 1614 (1994).
- [5] C.J. Camacho and D. Thirumalai, *Proc. Natl. Acad. Sci. USA* **90**, 6369 (1993).
- [6] D.K. Klimov and D. Thirumalai, *Proteins: Structure, Function and Genetics* **26**, 411 (1996).
- [7] N.D. Soccia and J.N. Onuchic, *J. Chem. Phys.* **101**, 1519 (1994); *ibid* **103**, 4732 (1995).
- [8] I. Srivastava *et al.*, *Proc. Natl. Acad. Sci. USA* **92**, 9206 (1995).
- [9] W. Kauzmann, *Adv. Protein Chem.* **14**, 1 (1959). For a recent review, see K.A. Dill, *Biochemistry* **29**, 7133 (1990).
- [10] H. Li, C. Tang, and N. Wingreen, *Phys. Rev. Lett.* **79**, 765 (1997).
- [11] S. Miyazawa and R. Jernigan, *Macromolecules* **18**, 534 (1985); *J. Mol. Biol.* **256**, 623 (1996).
- [12] S. Kamtekar, J.M. Schiffer, H. Xiong, J.M. Babik, and M.H. Hecht, *Science* **262**, 1680 (1993).
- [13] H. Li, R. Helling, C. Tang, and N. Wingreen, *Science* **273**, 666 (1996).
- [14] M. Vendruscolo, A. Maritan, and J.R. Banavar, *Phys. Rev. Lett.* **78**, 3967 (1997).
- [15] A.B. Bortz, M.H. Kalos, and J.L. Lebowitz, *Jour. Comp. Phys.* **17**, 10 (1975).
- [16] A.M. Ferrenberg and R.H. Swendsen, *Phys. Rev. Lett.* **63**, 1195 (1989).
- [17] The Ferrenberg-Swendsen multiple histogram method was applied to protein folding in Z. Guo and C.L. Brooks III, *Biopolymers* **42**, 745 (1997) and D.K. Klimov and D. Thirumalai, *Folding & Design* **3**, 127 (1998).
- [18] R.A. Goldstein, Z.A. Luthey-Schulten, and P. G. Wolynes, *Proc. Natl. Acad. Sci. USA*, **89**, 4918 (1992).
- [19] G.A. Petsko and D. Ringe, *Ann. Rev. Biophys. Bioeng.* **13**, 331 (1984).
- [20] J.D. Bryngelson and P.G. Wolynes, *Proc. Natl. Acad. Sci. USA* **84**, 7524 (1987); *Biopolymers* **30**, 171 (1990).

- [21] H. Li, C. Tang, and N. Wingreen, Proc. Natl. Acad. Sci. USA **95**, 4987 (1998).
- [22] H. Li, R. Helling, C. Tang, and N. Wingreen, unpublished.
- [23] V.I. Abkevich, A.M. Gutin, and E.I. Shakhnovich, J. Mol. Biol. **252**, 460 (1995).
- [24] J.D. Bryngelson and P.G. Wolynes, J. Phys. Chem. **93**, 6902 (1989).
- [25] J.D. Bryngelson, J.N. Onuchic, N.D. Soccia and P. Wolynes, PROTEINS: Structure, Function, and Genetics **21**, 167 (1995).
- [26] V.I. Abkevich, A.M. Gutin, and E.I. Shakhnovich, Biochemistry **33**, 10026 (1994).